Molecular Cell, Volume *62*

Supplemental Information

Recognition of Lys48-Linked Di-ubiquitin and Deubiquitinating Activities of the SARS Coronavirus Papain-like Protease

Miklós Békés, Gerbrand J. van der Heden van Noort, Reggy Ekkebus, Huib Ovaa, Tony T. Huang, and Christopher D. Lima

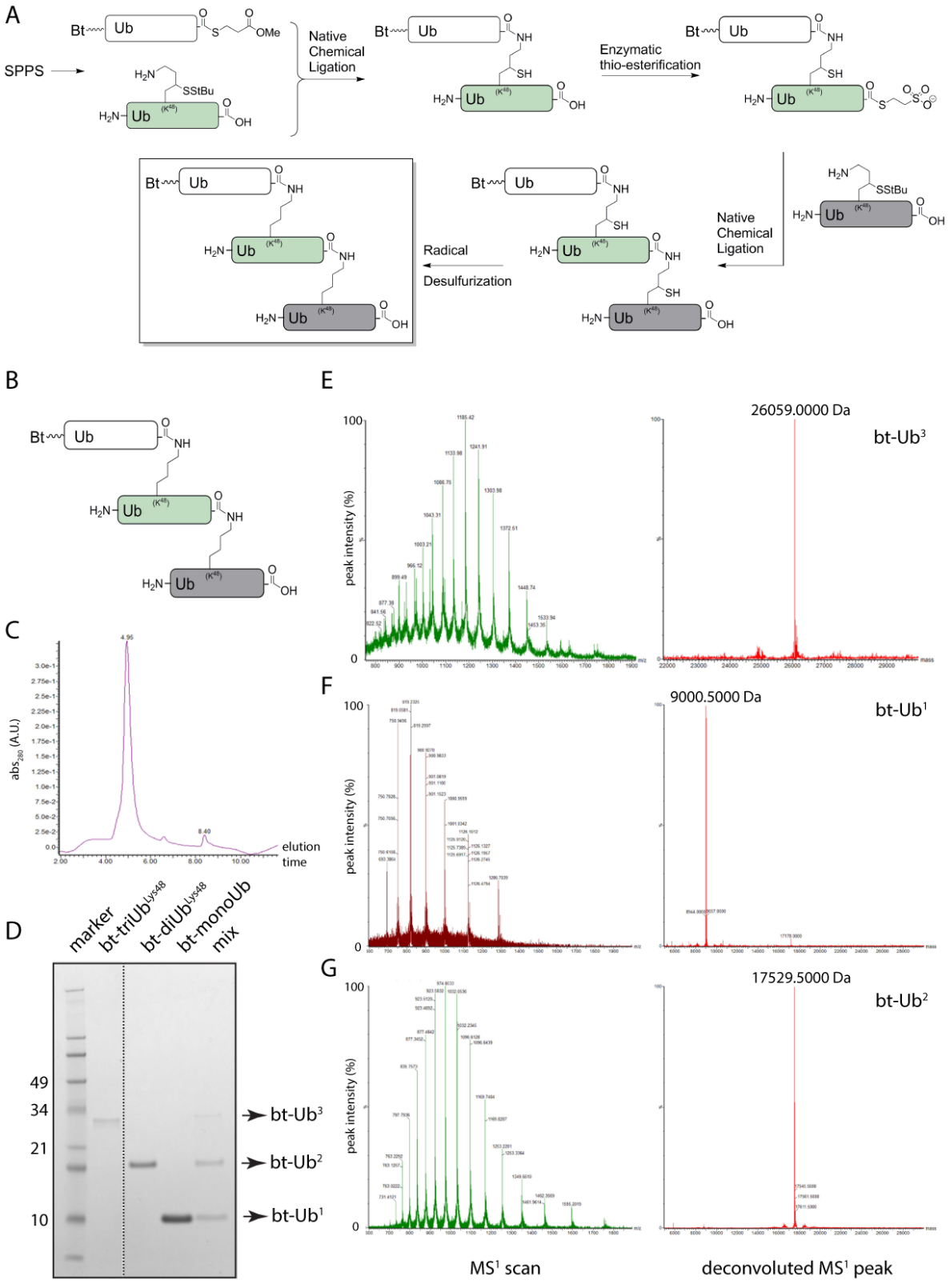

Figure S1 – related to Figure 1

A) Detailed synthesis scheme to obtain the native tri-ubiquitin^{Lys48} substrate carrying a single biotin tag on the N-terminus of the distal ubiquitin moiety. B) Schematics of the final biotin-triUb^{Lys48} substrate. C) LC-MS chromatography UV-profile of the final bt-triUb^{Lys48} product. D) Coommassie-stained SDS-PAGE analysis of the final bt-triUb^{Lys48} substrate, along with biotin-tagged mono- and diUb^{Lys48} controls. E-G) MS^1 analysis (on the left) and deconvoluted mass spectra (on the right) of bt-triUb^{Lys48} (E), bt-monoUb (F), and bt-diUb^{Lys48} (G).

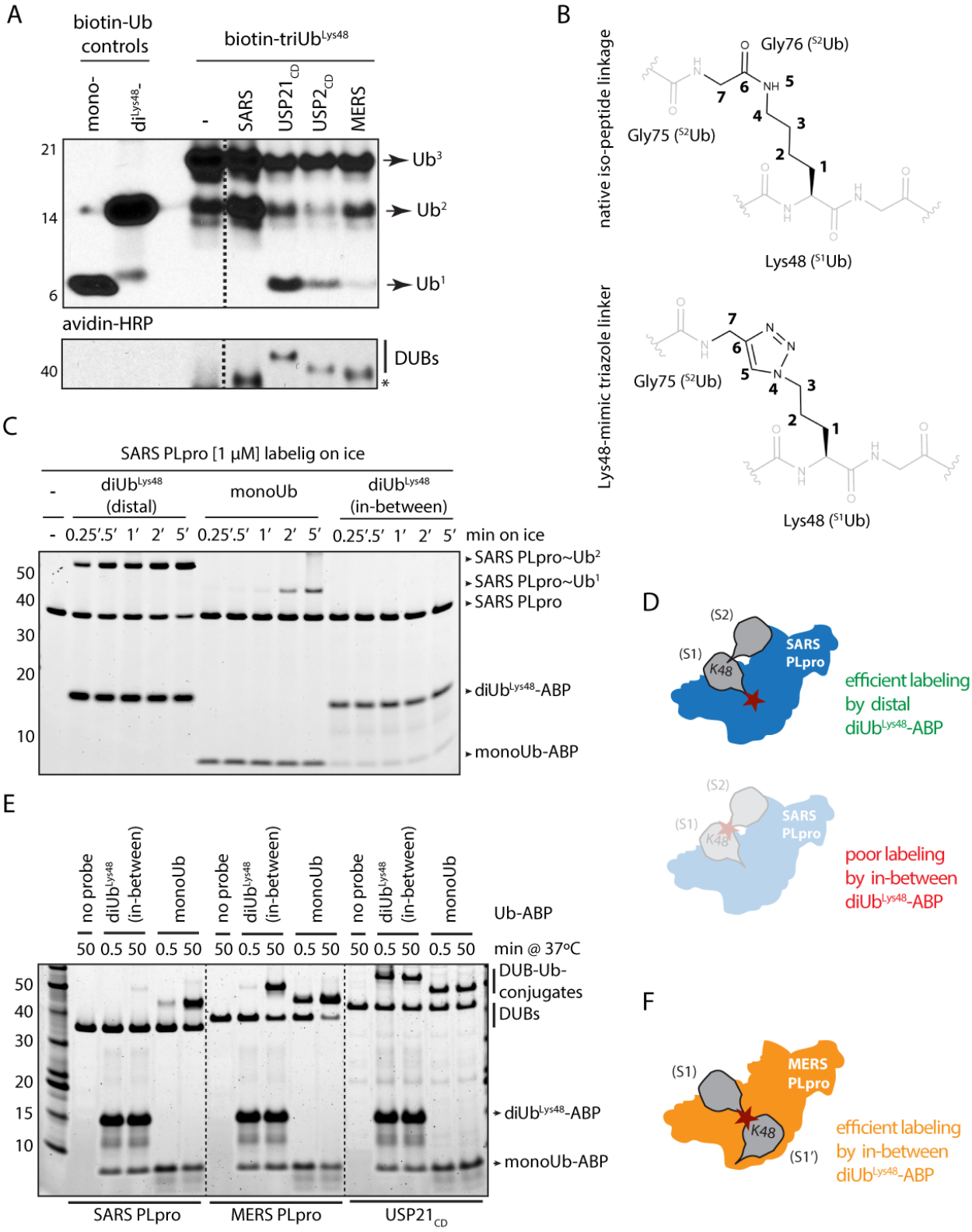

Figure S2 – related to Figure 1

A) Cleavage of biotin-triUb^{Lys48} by various DUBs [100 nM] for 15 min at 37ºC. Notice that the biotin-tag can be visualized on both mono- and diUb products for USP21$_{CD}$, UPS2$_{CD}$ and MERS PLpro, while it remains visible only on the diUb^{Lys48} product for SARS PLpro. B) Comparison of the chemical structure of a native isopeptide-bond (top) and the isosteric triazole linkage used in the distal diUb^{Lys48}-ABP (bottom). The number of atoms between the main-chain C-α of Lys48 of ^{S1}Ub and the main chain nitrogen of Gly75 of ^{S2}Ub is shown in bold, indicating similar distance and geometry of the triazole mimic. C) Representative gels of quantitative labeling assays of SARS PLpro by Ub-ABPs on ice used to generate Figure 1F. D) Schematics of SARS PLpro labeling by diUb-ABPs. E) Qualitative labeling assay of USP-family DUBs by the in-between diUb^{Lys48}-ABP. F) Schematics of diUb-ABP labeling for the related MERS PLpro, a monoUb-based DUB.

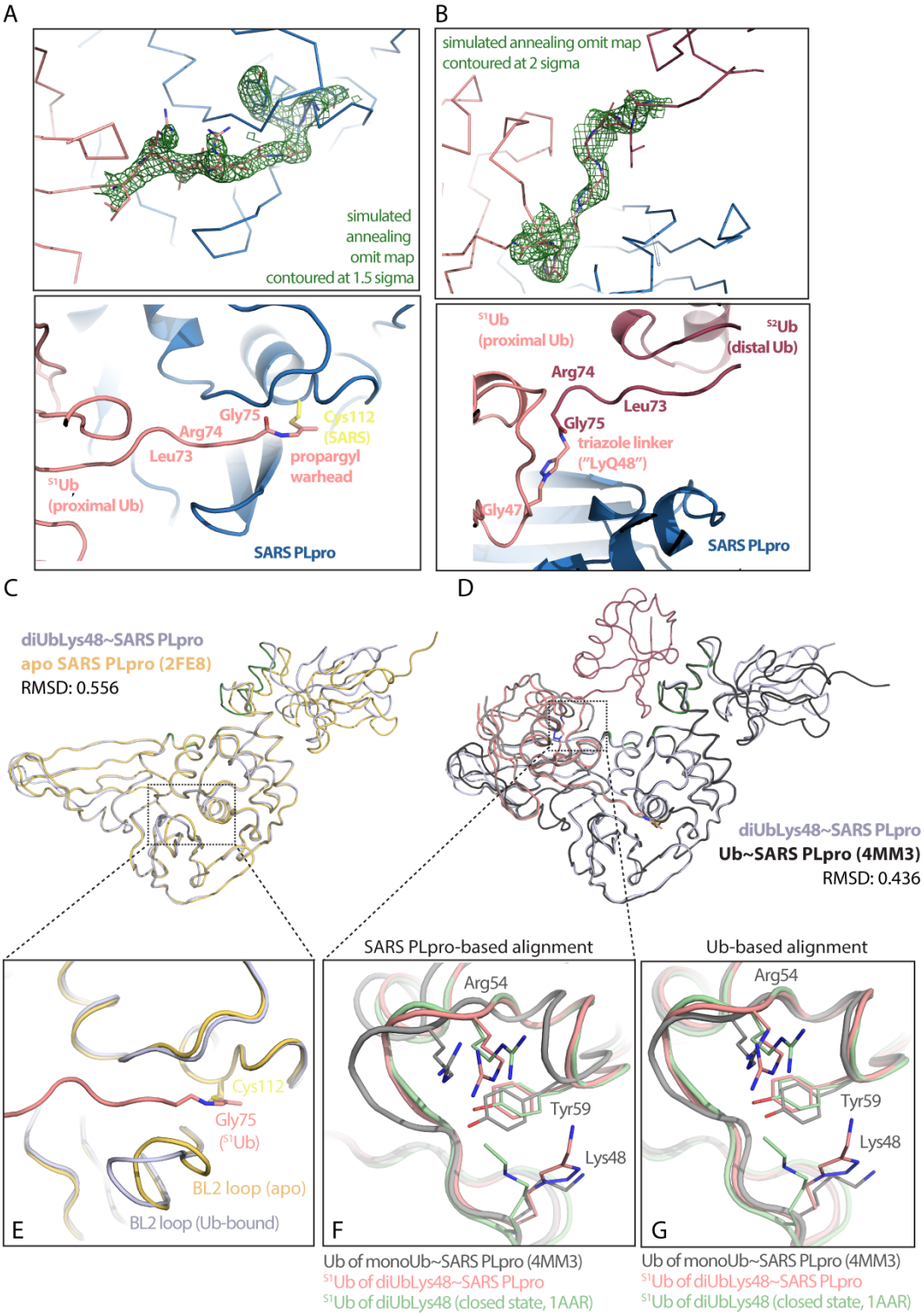

Figure S3 – related to Figure 2

A) Simulated annealing omit map contoured at 1.5σ (top) and cartoon representation (bottom) of the covalent linkage by the propargyl warhead between ^{S1}Ub-Gly75 and SARS-PLpro-Cys112. B) Simulated annealing omit map contoured at 2σ (top) and cartoon representation (bottom) of the covalent linkage by the triazole linker between ^{S2}Ub-Gly75 and ^{S1}Ub-Lys48. C) Cartoon representation of the structure-based alignment of SARS PLpro from the diUb^{Lys48} complex (in blue-white) and the apo SARS PLpro structure (PDB 2FE8, in wheat (Ratia et al., 2006)). D) Structure-based alignment of SARS PLpro from the diUb^{Lys48} complex (in blue-white) and from the monoUb-aldehyde complex (PDB 4MM3, SARS in black, Ub in grey (Ratia et al., 2014)). E) Detail of the alignment in C), showing orientation of the BL2 loop. E-G) Structure-based alignment of the diUb^{Lys48}-SARS complex with free diUb^{Lys48} (PDB 1AAR (Cook et al., 1992)) and the SARS monoUb complex (4MM3). In F), alignment was performed based on the SARS DUB domain; in G) alignment was performed based on the proximal Ub.

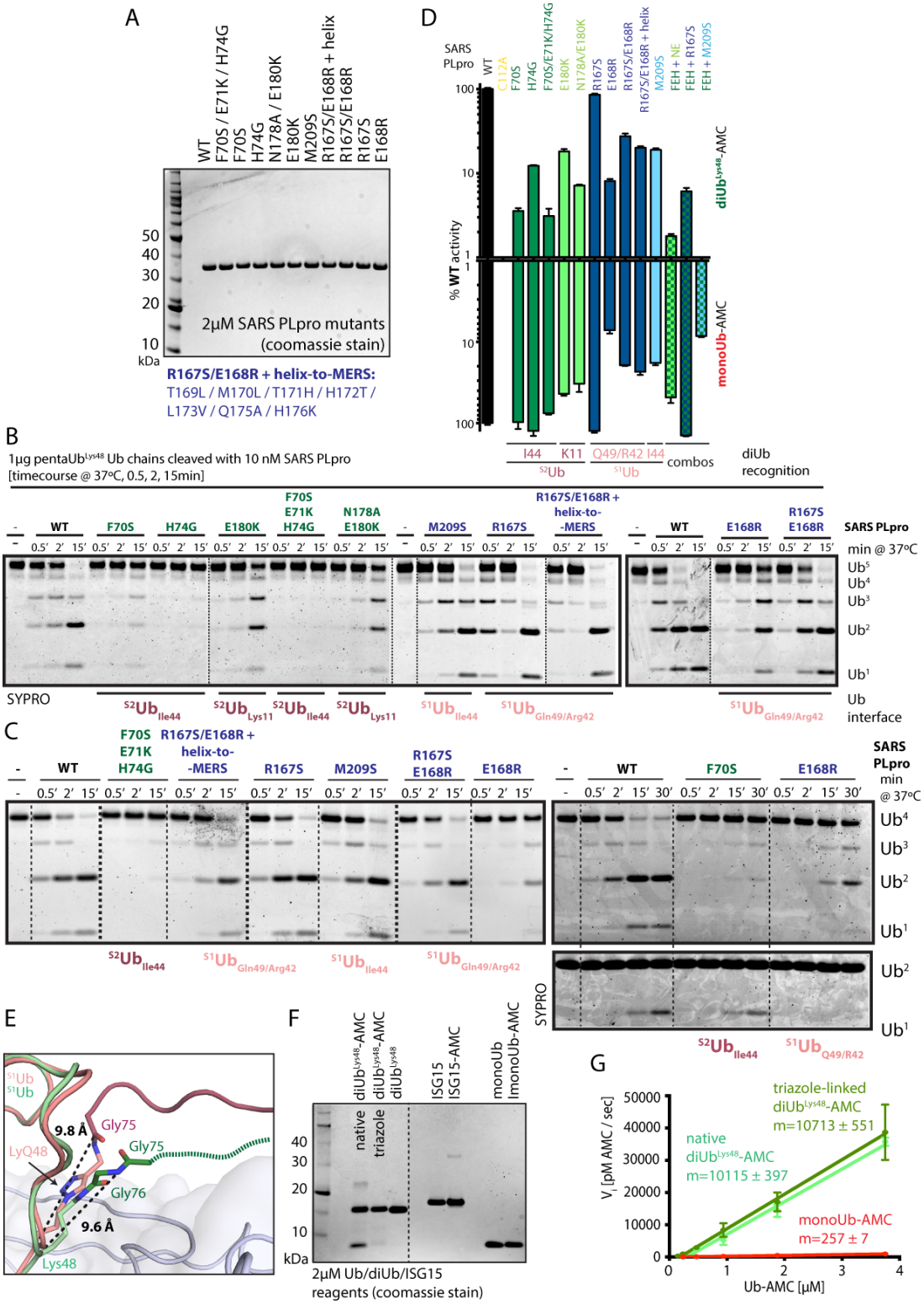

Figure S4 – related to Figure 3

A) Purified SARS PLpro mutants (2 μM) analyzed by SDS-PAGE and coomassie staining. B) Representative gels used to monitor pentaUb^{Lys48} cleavage activity of SARS PLpro mutants shown in Figure 3A. Dotted lines indicate cropping between gels. C) Qualitative cleavage assay of tetra- and diUb^{Lys48} by 10 nM and 50nM SARS PLpro mutants, respectively. Light dotted lines are included for clarity; heavy dotted lines indicate cropping between gels. D) Initial cleavage of SARS PLpro WT (in black), its ^{S2}Ub (in green), its ^{S1}Ub (in blue) and combination mutants on diUb^{Lys48}-AMC (top panel, triazole-linked) and monoUb-AMC (bottom panel) substrates, expressed as percent of WT activity. Error bars represent ±SEM. E) Structure-based alignment of the diUb^{Lys48}-SARS complex with free diUb^{Lys48} (PDB 1AAR), showing the geometry and distance of the triazole-linker compared to the native isopeptide-linkage. F) Coomassie gel of Ub-reagents used in this study for kinetic and inhibition analysis, which is shown in Table 2. G) Initial cleavage rates of triazole-linked (dark green line) and native (light green line) diUb^{Lys48}-AMC substrates by SARS PLpro.

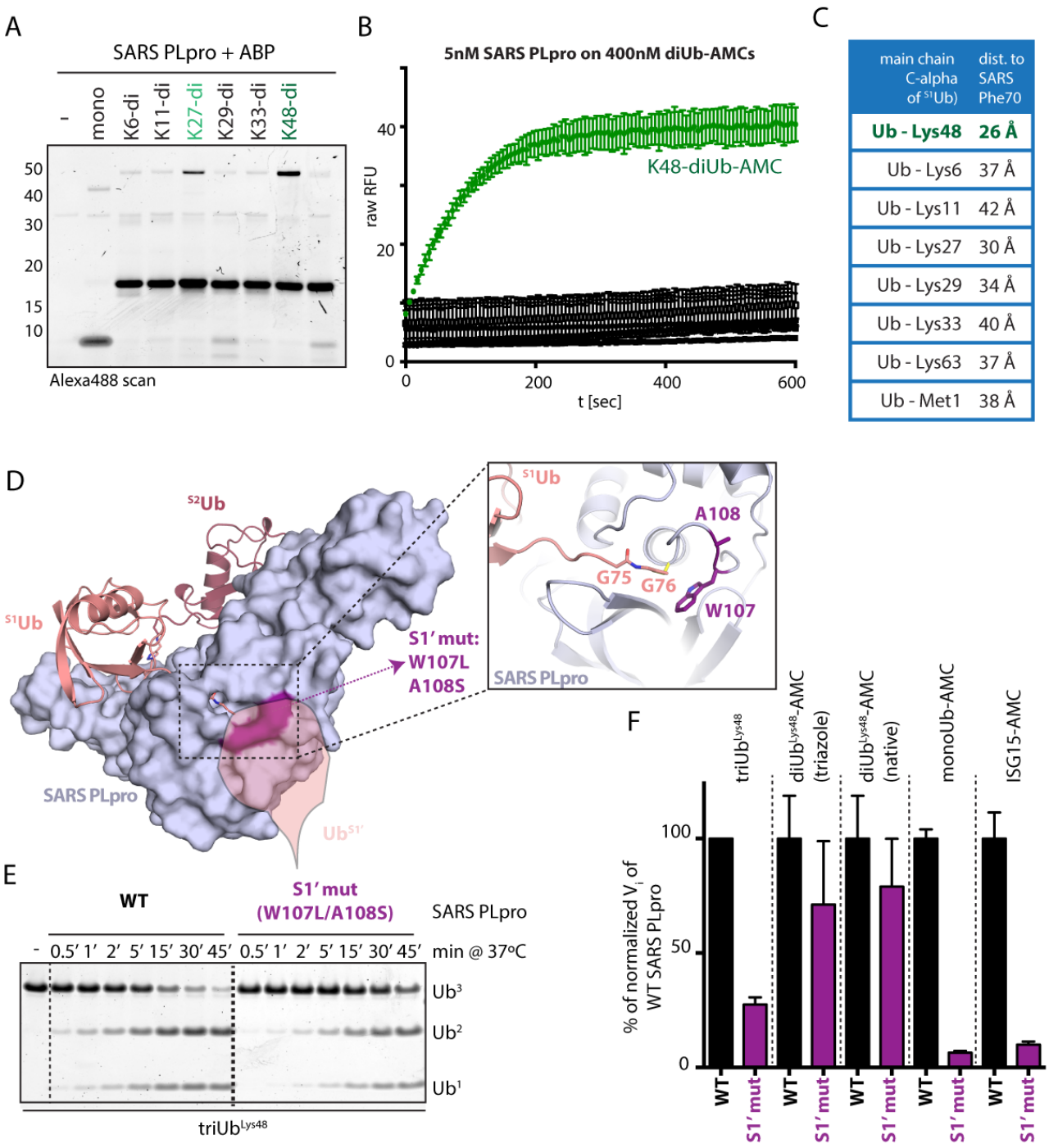

Figure S5 – related to Figure 4

A) Labeling assay of SARS PLpro with linkage-specific diUb-ABPs at 37ºC for 30 sec (as shown in Figure 4A), visualized by Alexa488-scan (at 488 nm) to reveal the diUb probes. B) Example raw relative fluorescence unit (RFU) progress curves for linkage-specific diUb-AMC substrate cleavage reactions. Triplicates of such reactions were used to generate Figure 4B; in green is the diUb^{Lys48}-AMC; in black are all other -AMC substrates. C) Distances (in Å) between the main-chain C-α of each Ub chain forming residue of ^{S1}Ub to Phe70 of the ^{S2}Ub binding site in SARS PLpro. D) Structure-based representation of a putative S1' mutant – W107L/A108S – shown in purple; the inset shows a zoom for the active site of SARS PLpro, Trp107 and Ala108 are shown as sticks. E) Gel-based cleavage assay of 10nM SARS PLpro WT versus the W107L/A108S mutant. Initial cleavage rates are quantified in Supplementary Figure 5F (first panel). F) TriUb^{Lys48} cleavage rates (from Supplementary Figure 5E) expressed as percent of WT, compared to cleavage rates of WT and the W107L/A108S mutant on triazole-linked and native diUb^{Lys48}-, monoUb- and ISG15-AMC substrates Error bars represent ±SEM, n=2 for triUb^{Lys48}, n=4 for monoUb-, diUb^{Lys48}(native and triazole-linked)- and ISG15-AMC substrates.

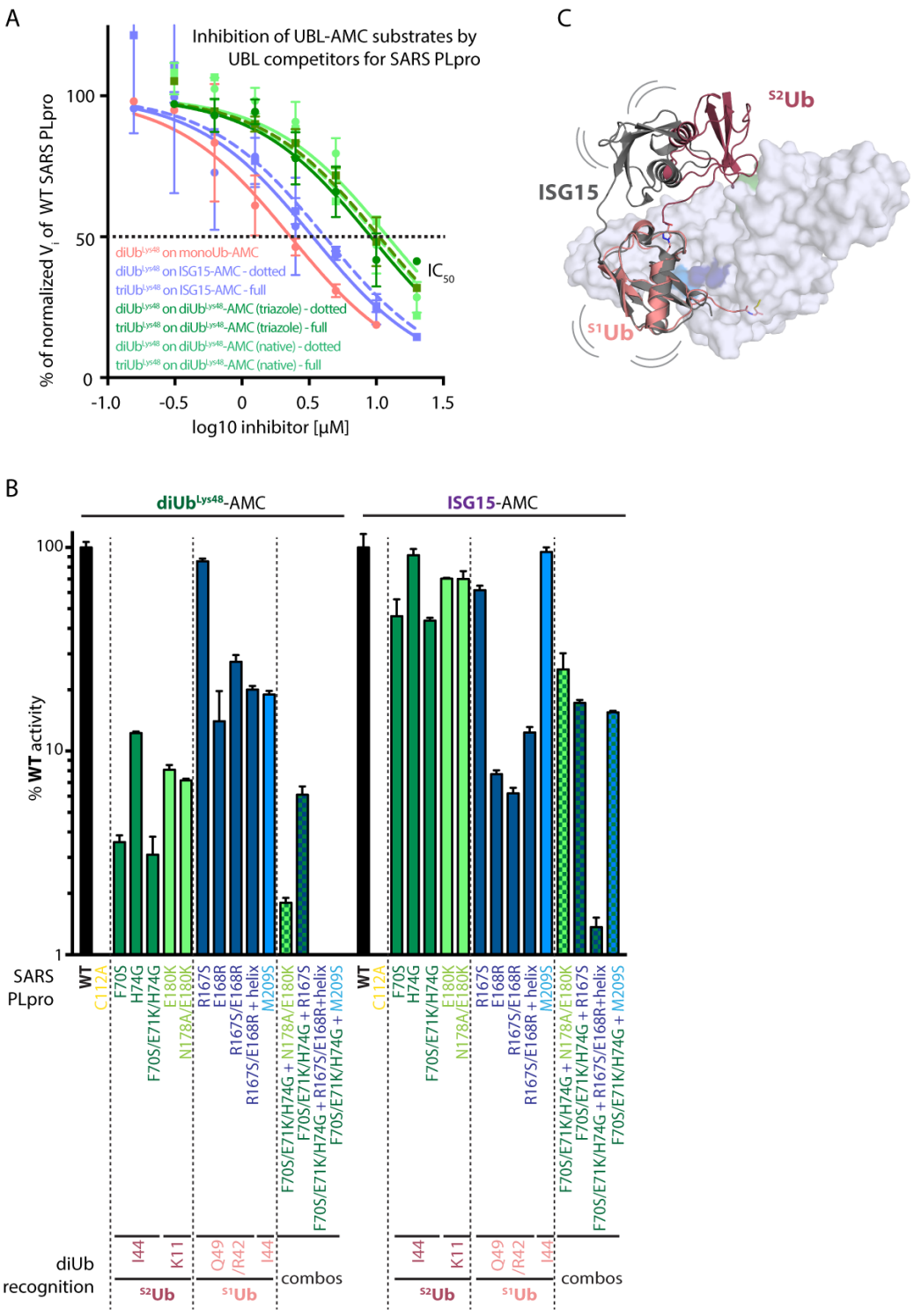

Figure S6 – related to Figure 5 and Table 2

A) Inhibition assays of Ub-based inhibitors on Ubl-AMC substrates graphed as IC_{50} values, showing percent of no inhibitor cleavage rates at each inhibitor concentration. IC_{50} values were transformed into K_i values (Cer et al., 2009) and are shown in Table 2. Dark green full line – $diUb^{Lys48}$ on $diUb^{Lys48}$-AMC (triazole-linked); dark green dotted line – $triUb^{Lys48}$ on $diUb^{Lys48}$-AMC (triazole-linked); light green full line – $diUb^{Lys48}$ on $diUb^{Lys48}$-AMC (native); light green dotted line – $triUb^{Lys48}$ on $diUb^{Lys48}$-AMC (native); purple full line – $diUb^{Lys48}$ on ISG15-; purple dotted line – $triUb^{Lys48}$ on ISG15-AMC; pink full line – $diUb^{Lys48}$ on monoUb-AMC. B) Activity of SARS PLpro and its mutants on ISG15-AMC hydrolysis (compared to $diUb^{Lys48}$-AMC, data for $diUb^{Lys48}$-AMC are taken from Supplemental Figure 4D). C) Modeling of ISG15 (in grey, PDB 1Z2M) bound to SARS PLpro by aligning its proximal Ub-like domain to ^{S1}Ub in the SARS-PLpro~$diUb^{Lys48}$ complex. Curved lines indicate the presumed flexibility of the ISG15. Dotted lines are included for clarity. Error bars represent ±SEM.

SUPPLEMENTAL EXPERIMENTAL PROCEDURES

Synthesis of the singly-biotinylated triUb^{Lys48} substrate

The singly biotin-tagged triUb^{Lys48} chain substrate was generated using a combination of native chemical ligation reactions, enzymatic thio-esterification and radical desulfurization on synthetically produced Ub thio-ester- and thiolysine-mutants (Merkx et al., 2013). Briefly, synthetic N-terminally biotinylated Ub thioester (25 mg/mL) and synthetic K48-thiolysine Ub (25 mg/mL) were ligated in 8 M Gdn.HCl / 200 mM NaH_2PO_4, pH 7.6 in the presence of 1.2 M mercaptophenyl acetic acid (MPAA) for 16 hours at 37^{o}C. After HPLC and size exclusion chromatography (SEC), the resulting Bt-diUb^{Lys48} C-terminal carboxylic acid (13 mg/mL) was converted to its MESNa-thioester using recombinant UBA-E1 ubiquitin activating enzyme (250 nM) in 200 mM HEPES buffer, pH 7.7 containing 10 mM ATP, 10 mM $MgCl_2$ and 100 mM MESNa for 1 hour at 37^{o}C. After HPLC purification, the appropriate fractions were pooled and lyophilized to yield Bt-diUb^{Lys48}-MESNa, which was ligated to K48-thiolysine Ub (25 mg/mL) in 8 M Gdn.HCl/ 200 mM NaH_2PO_4, pH 7.6 in the presence of 1.2 M MPAA for 16 hours at 37^{o}C. After HPLC- and Size Exclusion Chromatography the resulting Bt-Ub$_3^{Lys48}$ was desulfurized in 8 M Gdn.HCl/200 mM NaH_2PO_4, pH 6.8 in the presence of 200 mM TCEP, 75 mM GSH (reduced form) and 75 mM of the radical initiator VA-044. Concomitant HPLC and subsequent SEC-purification resulted in the target compound: Bt-triUb^{Lys48}

Cloning, protein expression, purification and crystallization.

The generation of recombinant SARS and MERS PLpro has been previously described (Bekes et al., 2015). Briefly, the nucleotide sequence (nts 4451-7179) from MERS HCoV ORF1a (GenBank AGV08402.1) and the nucleotide sequence encoding the SARS PLpro minimal domain (nts 4884-5829, aa 1541-1885, PDB: 3MJ5) were gene synthesized by GenScript and subcloned into pET28b with a C-terminal 6xHis-tag. All mutations were generated by over-lapping PCR and verified by sequencing. DUBs (SARS and MERS PLpro and USP21$_{CD}$) were expressed in *E.coli* BL-21 codon plus RIL cells and purified until homogeneity as previously (Bekes et al., 2015). Briefly, *E.coli* was grown at 37ºC until OD_{600}=1.0 and induced with 1 mM IPTG and further incubated at 30ºC for 4 hours. Harvested cell pellets were flash frozen in liquid nitrogen and stored at -80ºC until purification. Frozen pellets were thawed on ice and lysed in 20 mM Tris, pH=8.0, 350 mM NaCl, 1 mM PMSF, 1 mM beta-mercaptoethanol, 1% NP-40 and 10 mM imidazole by sonication. After centrifugation, the supernatant was applied onto Ni-NTA resin (Quiagen) for batch-binding by rotation for 1 hour at 4ºC. Ni-bound DUBs were eluted with 20 mM Tris, pH=8.0, 350 mM NaCl, 250 mM imidazole and 1 mM beta-mercaptoethanol, concentrated and purified by size-exclusion chromatography on a Superdex-75 (16/600) column (GE); peak fractions were collected, concentrated to 1-10 mg/mL, aliquoted and stored at -80ºC until use. SARS PLpro mutants were purified by Ni-NTA purifications and buffer exchanged into assay buffer (20 mM Tris, pH=8.0, 150 mM NaCl using BioRad spin-columns and supplemented with 1 mM DTT prior to biochemical assays.

Structure Determination

X-ray diffraction data were processed using HKL2000 (Otwinowski, 1997), the statistics obtained by Phenix (Adams et al., 2010) are reported in Table 1. Crystals were in space group $P2_1$ with two complexes in the asymmetric unit. An initial structure solution was obtained by molecular replacement by Phaser (McCoy et al., 2007) using coordinates of the apo form of SARS PLpro (PDB 2FE8 (Ratia et al., 2006)), monoUb-bound SARS PLpro (PDB 4MM3 (Ratia et al., 2014)) and of monoUb (PDB 1UBQ), which model then subsequently underwent iterative refinement and further modeling in Coot (Emsley et al., 2010) to add the second Ub, manually model the propargyl warhead (between ^{S1}Ub-Gly75 and SARS PLpro-Cys112) and the triazole linkage (between ^{S1}Ub-Lys48 and ^{S2}Ub-Gly75) in the continuous electron density within the covalent complex. The two complexes in the ASU align with an RMS of 0.978 over 3350 atoms (SARS PLpro amino acids 4-316 and the two full-length Ub molecules). A final model with R_{work}/R_{free} of 23.2/26.4 at 2.85Å resolution was obtained with good geometry, as assessed by MolProbity (Chen et al., 2010), (with 93.3%, 99.7%, and 0.3% in favored, allowed, and disallowed regions of Ramachandran space, respectively). Figures showing the structure were generated using Pymol (The PyMOL Molecular Graphics System, version 1.5.0.4. Schrödinger, LLC.) The final model has the PDB code 5E6J.

Synthesis of mono- and diUb activity-based probes and -AMC derivative substrates with the triazole linkage

For generation and characterization of the non-hydrolyzable "distal" diUb activity-based probes and -AMC derivative substrates, please refer to the manuscript by Flierman et al. in Cell Chemical Biology (Flierman et al., 2016).

Synthesis of diUb-AMC substrates (native linkage)

DiUb^{Lys48} carrying a native isopeptide-linkage, equipped with a C-terminal 7-amido-4-methyl-coumarine (AMC) was generated using a procedure based on a previously reported native chemical ligation protocol (El Oualid et al., 2010) as described above, starting from synthetic Ub thioester and synthetic K48-thiolysine Ub-AMC.

Biotin-triUb^{Lys48} cleavage assays

In a reaction volume of 10 µL, 0.5 µg biotin-triUb^{Lys48} substrate (in 20 mM Tris, pH 8.0, 150 mM NaCl and 5 mM DTT) was cleaved with 100 nM DUBs for 5 min at 37ºC or with a 1/5-serial dilution of SARS PLpro starting at 500 nM. Reactions were terminated with loading buffer (4X LDS, Invitrogen), boiled for 5min at 95ºC (the standard protocol for

SDS-PAGE) split into two and analyzed in parallel by SDS-PAGE and SYPRO-staining; and by SDS-PAGE, then transferred to PVDF membranes and incubated with streptavidin-HRP. Biotin-labeled Ub cleavage products were visualized by chemiluminescence, blots were developed by film.

Inhibition assays using fluorogenic substrates

To determine IC_{50} values, a fixed concentration of monoUb-, $diUb^{Lys48}$-AMC or ISG15-AMC at 200 nM was mixed at 25ºC with a 2-fold serial dilution of inhibitor (starting at 15 or 30 μM), then mixed immediately with 5-50 nM SARS PLpro in a final volume of 15 μL. Inhibition assays were performed at 30ºC using a Spectramax fluorescence plate reader running SoftMax Pro 5 (Molecular Devices) operated in kinetic mode, in black, round-bottom 384-well plates (Corning #3698), where free AMC fluorescence was monitored by excitation at 355 nm and emission at 460 nm over time for 5-10 min. Initial linear cleavage rates (V_i) were expressed as percent of no inhibitor cleavage rate for every run and were fitted to Prism's log(inhibitor) vs. normalized curve equation, which calculated IC_{50} values. IC_{50} were then transformed into K_i values based on the equation $K_i = IC_{50}/(S/K_M+1)$, assuming low affinity, competitive inhibition, where S is the concentration of the substrate (*Cer et al. 2009, NAR*). Kinetic and inhibition parameters are presented in Table 2.

Commercial reagents

Ub chains, Ub-AMC and ISG15-AMC were purchased from Boston Biochem. Antibodies used in this study were anti-ISG15 (#2743 from Cell Signaling), anti-Ub (P4D1, sc-8017 from Santa Cruz Biotech), anti-His (in-house, gift of D. Reinberg, NYUMC), anti-IκBα (C-21, Santa Cruz Biotech), and anti-K48-linkage (Apu2, Millipore). Streptavidin-HRP was purchased from GE Healthcare (#RPN123V).

Cell culture and cell lysate preparation

HeLa cells were cultured by standard cell culture technique, in DMEM with glutamine, penicillin/streptomycin, and 10% FBS at 37ºC with 5% CO_2. Cells were left untreated or treated with 500 units/mL of interferon-beta (human IFNβ1a, purchased from PBL Interferon Source, product #1141501) for 48 hours at 37ºC and the proteasome inhibitor MG132 (10 μM, Calbiochem) was included for the last 4 hours in the cell culture before harvest. For TNF-α treatments, HeLa cells were pre-treated with fresh media containing 10 μM MG132 for 30 min at 37ºC, then 10 ng/mL TNF-α was added directly to the media and cells were incubated for another 15 min at 37ºC. Cells were immediately harvested by scraping in cold PBS and pellets were frozen at -80ºC. Pellets were lysed on ice for 1 hour in 50 mM Tris, pH=7.5, 150 mM NaCl, 1 mM EDTA, 0.5% NP-40 in the presence of a protease inhibitor cocktail (Roche), 1 mM 1,10-phenantroline and 20 mM N-ethyl-maleimide to preserve Ub conjugates. DNA was cleared by the addition of benzoase (Novagen). The supernatant was cleared by centrifugation, and lysates were quantified using a BioRad Protein Assay by measuring absorbance at 595 nm.

SUPPLEMENTAL REFERENCES

Adams, P.D., Afonine, P.V., Bunkoczi, G., Chen, V.B., Davis, I.W., Echols, N., Headd, J.J., Hung, L.W., Kapral, G.J., Grosse-Kunstleve, R.W., *et al.* (2010). PHENIX: a comprehensive Python-based system for macromolecular structure solution. Acta Crystallogr D Biol Crystallogr *66*, 213-221.

Bekes, M., Rut, W., Kasperkiewicz, P., Mulder, M.P., Ovaa, H., Drag, M., Lima, C.D., and Huang, T.T. (2015). SARS hCoV papain-like protease is a unique Lys48 linkage-specific di-distributive deubiquitinating enzyme. Biochem J *468*, 215-226.

Cer, R.Z., Mudunuri, U., Stephens, R., and Lebeda, F.J. (2009). IC50-to-Ki: a web-based tool for converting IC50 to Ki values for inhibitors of enzyme activity and ligand binding. Nucleic Acids Res *37*, W441-445.

Chen, V.B., Arendall, W.B., 3rd, Headd, J.J., Keedy, D.A., Immormino, R.M., Kapral, G.J., Murray, L.W., Richardson, J.S., and Richardson, D.C. (2010). MolProbity: all-atom structure validation for macromolecular crystallography. Acta Crystallogr D Biol Crystallogr *66*, 12-21.

Cook, W.J., Jeffrey, L.C., Carson, M., Chen, Z., and Pickart, C.M. (1992). Structure of a diubiquitin conjugate and a model for interaction with ubiquitin conjugating enzyme (E2). J Biol Chem *267*, 16467-16471.

El Oualid, F., Merkx, R., Ekkebus, R., Hameed, D.S., Smit, J.J., de Jong, A., Hilkmann, H., Sixma, T.K., and Ovaa, H. (2010). Chemical synthesis of ubiquitin, ubiquitin-based probes, and diubiquitin. Angew Chem Int Ed Engl *49*, 10149-10153.

Emsley, P., Lohkamp, B., Scott, W.G., and Cowtan, K. (2010). Features and development of Coot. Acta Crystallogr D Biol Crystallogr *66*, 486-501.

Flierman, D., van der Heden van Noort, G.J., Ekkebus, R., Geurink, P.P., Mevissen, T.E., Hospenthal, M.K., Komander, D., and Ovaa, H. (2016). Non-hydrolyzable Diubiquitin Probes Reveal Linkage-Specific Reactivity of Deubiquitylating Enzymes Mediated by S2 Pockets. Cell Chem Biol *23*, 472-482.

McCoy, A.J., Grosse-Kunstleve, R.W., Adams, P.D., Winn, M.D., Storoni, L.C., and Read, R.J. (2007). Phaser crystallographic software. Journal of applied crystallography *40*, 658-674.

Merkx, R., de Bruin, G., Kruithof, A., van den Bergh, T., Snip, E., Lutz, M., El Oualid, F., and Ovaa, H. (2013). Scalable synthesis of gamma-thiolysine starting from lysine and a side by side comparison with delta-thiolysine in non-enzymatic ubiquitination. Chem Sci *4*, 4494-4498.

Otwinowski, Z.M., W. (1997). Methods in Enzymology (eds Carter, C. W. Jr. & Sweet, R. M.) *276*, 307-326.

Ratia, K., Kilianski, A., Baez-Santos, Y.M., Baker, S.C., and Mesecar, A. (2014). Structural Basis for the Ubiquitin-Linkage Specificity and deISGylating activity of SARS-CoV papain-like protease. PLoS pathogens *10*, e1004113.

Ratia, K., Saikatendu, K.S., Santarsiero, B.D., Barretto, N., Baker, S.C., Stevens, R.C., and Mesecar, A.D. (2006). Severe acute respiratory syndrome coronavirus papain-like protease: structure of a viral deubiquitinating enzyme. Proc Natl Acad Sci U S A *103*, 5717-5722.